

## Supplementary Online Material

### Electric-field-induced polar order and charge localisation in LaAlO<sub>3</sub>/SrTiO<sub>3</sub> heterostructures

#### Infrared ellipsometry response of SrTiO<sub>3</sub>

Figure S1 shows the infrared response of SrTiO<sub>3</sub> at representative temperatures of 10 and 300 K as measured with ellipsometry on a commercially available single crystalline substrate (Crystec). Figure S1(a) display the ellipsometric angles  $\Psi$  and  $\Delta$  at an incidence angle of 80° and Figure S1(b) the derived real part of the optical conductivity. The black arrows mark the eigenfrequencies of the transverse-optical (TO) infrared-active phonon modes of the cubic phase at 300 K. These are the soft mode at  $\sim 95 \text{ cm}^{-1}$  (which decreases to  $\sim 15 \text{ cm}^{-1}$  at 10 K), the external mode at  $175 \text{ cm}^{-1}$ , and the bending mode at  $544 \text{ cm}^{-1}$ . The red arrow indicates the R-mode which develops below the anti-ferrodistortive phase transition at 105 K where the crystal structure becomes tetragonal. The temperature and electric field dependence of this R-mode is shown in detail in Figs. 1(d)-(g) and 2(c) and 2(d) of our paper. The grey arrow indicates the position of the highest longitudinal optical (LO) mode at  $\sim 860 \text{ cm}^{-1}$ .

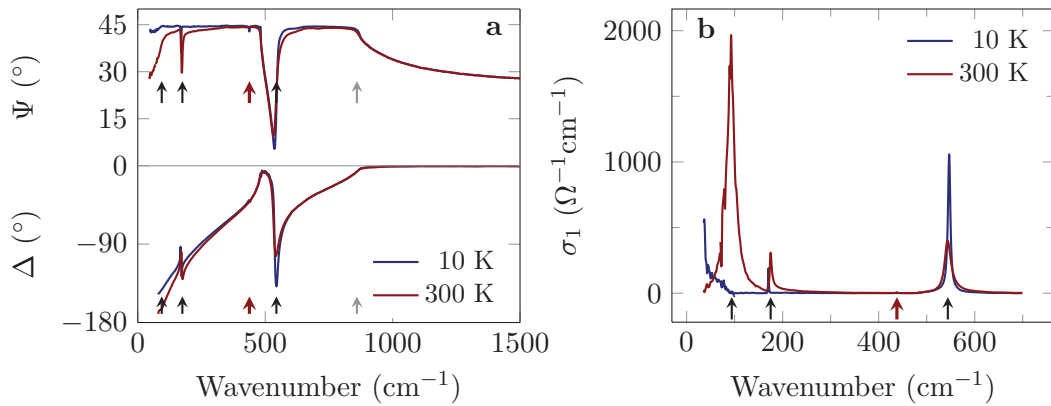


Figure S1: Ellipsometry spectra of a SrTi<sup>16</sup>O<sub>3</sub> crystal at 10 and 300 K, respectively. **a**, Ellipsometric angles  $\Psi$  and  $\Delta$  and **b**, derived optical conductivity  $\sigma_1$ . Note the different energy ranges. The black arrows indicate the phonon eigenfrequencies of the cubic phase at 300 K. The red arrow marks the R-mode which becomes weakly IR-active in the tetragonal phase below 105 K. The position of the highest LO mode (the so-called LO edge) is marked by the grey arrow in **a**.

## List of the samples

Table S1 gives an overview of the LAO/STO heterostructures and the measurements which have been performed. The nominal thickness of the LAO layer is given in terms of the number of unit cells. The “++” symbol in the column FIR indicates that a sizeable electric field induced anomaly (splitting) of the  $R$ -mode has been observed. A weak phonon anomaly is indicated by the “+” sign. The “0” sign indicates that no such anomaly of the  $R$ -mode has been observed for voltages  $V_g \leq \pm 250$  V. The FIR spectra showing the relatively weak field-induced anomaly of the  $R$ -mode in sample LS3.1 are displayed in Figure S2. The sample Ti-STO is a STO substrate that has been coated with a  $\sim 4$  nm thick Ti layer. It exhibits no sign of a field-induced anomaly of the  $R$ -mode in the measured range of  $V_g \leq \pm 250$  V. A shift of the LO edge is observed in the MIR ellipsometry spectra as discussed later and shown in Figure S4 for samples with  $n \geq 4$ . A strong shift of the LO edge is marked with “++” and “0” indicates that no shift of the LO edge has been observed as function of the applied gate voltage of  $V_g \pm 250$  V.

Table S1: Overview of the measurements that have been performed on the LAO/STO heterostructures. The thickness of the LAO layer is given in terms of the number of unit cells.

sample name	LAO thickness (uc)	FIR	MIR	X-ray	Resistance
LS-5.5_1	5.5	++	++	√	√
LS-3.1	3	+	0	–	–
LS-5.5_2	5.5	++	–	–	–
LS-4.5	4.5	++	++	–	–
LS-3.2	3	+	–	–	–
Ti-STO	0	0	–	–	–

## Field-dependent ellipsometry spectra of samples with a LAO layer thickness of 3 unit cells

Figure S2 shows the gate-voltage-dependence of the  $R$ -mode in the optical conductivity as measured with far-infrared ellipsometry on the LAO/STO heterostructures LS-3.1. Only a faint signature of a splitting and softening of the  $R$ -mode is observed here. The onset of this anomaly occurs at a gate voltage of  $\sim -150$  V which is considerably higher than in LS-5.5\_1 as shown in Figure 1(d) of the manuscript. As compared to the spectra of LS-5.5\_1 in Fig. 1(d) and 1(e) of the manuscript, the intensity reduction of the original mode at  $438 \text{ cm}^{-1}$  is weaker and the field-induced, additional peaks are less pronounced.

Accordingly, for the LS-3.1 sample it is difficult to determine the peak positions and thus the magnitude of the splitting of the  $R$ -mode.

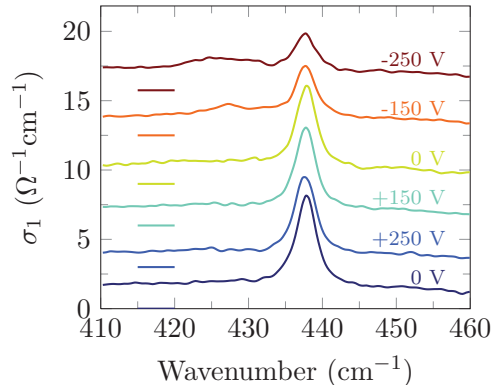


Figure S2: Field-dependent optical conductivity spectra of LS-3.1 which have been obtained at  $T = 10$  K. The  $R$ -mode shows only a weak and broad additional feature as a negative gate voltage is applied to the heterostructure.

### Polarisation of $\text{SrTiO}_3$ along the $[110]_c$ or $[111]_c$ axes

In Fig. 1(c) of the paper we show a sketch of the ferroelectric polarisation due to a displacement for the Ti cations along the crystallographic  $[001]_c$  direction (in cubic notation). Other possible Ti displacements are discussed in the following.

A shift of the Ti cation along the  $[110]_c$  direction is schematically shown in Figure S3(a). Two of the Ti-O bonds are shortened and their eigenfrequency is blue-shifted here whereas four bonds are elongated and their eigenfrequencies are red-shifted as indicated by the colours of the bonds, respectively. Similar to the case of the  $[001]_c$  displacement described in the paper, the  $R$ -mode thus also becomes anisotropic and splits into two branches corresponding to rotations and movements that involve either one blue and three red bonds or two blue and two red bonds, respectively.

It has recently been argued in Ref. [1] that such a  $[110]_c$  displacement occurs in the ferroelectric state of  $\text{SrTi}^{18}\text{O}_3$  for which the anomaly of the  $R$ -mode is shown in Figs. 2(a) and 2(b) of the paper.

The third possible scenario is shown in Figure S3(b) where the Ti atom is displaced along the  $[111]_c$  direction. This results in an equal number of three shorter and three longer bonds for which the  $R$ -mode remains isotropic. This case does not seem to be realised in  $\text{SrTi}^{18}\text{O}_3$  nor in the LAO/STO heterostructures where the  $R$ -mode exhibits a clear splitting and therefore becomes anisotropic as is discussed in the manuscript.

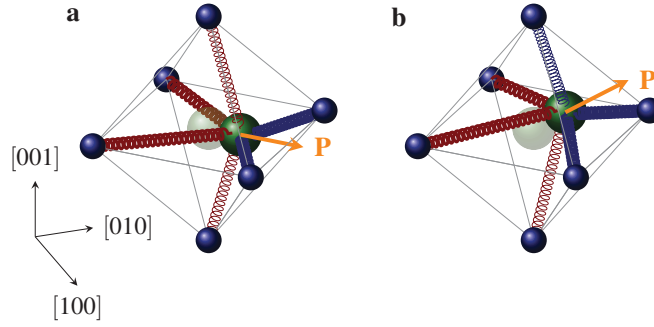


Figure S3: **a**, Sketch of the (exaggerated) polar displacement of the central Ti atom in a  $\text{TiO}_6$  octahedron of STO along the  $[110]_c$  axis and **b**, along the  $[111]_c$  axis. The resulting polarisation is indicated by the orange vectors.

## Modelling of the R-mode at negative gate voltage

For the fitting of the split *R*-mode at  $V_g = -250$  V in Figure 1(d) the following procedure has been applied. At first we have performed a fit of the spectrum at  $+250$  V where only the *R*-mode due to the paraelectric  $\text{SrTiO}_3$  is present. This fit was performed using three Lorentz oscillators, one for the *R*-mode at  $438\text{ cm}^{-1}$  and one each for the soft mode at very low frequency and the stretching mode at  $\sim 540\text{ cm}^{-1}$  that are both well outside the spectral range that is shown in Fig. 1(d). The same modes and parameters were then subsequently used to account for the response of the paraelectric part of the  $\text{SrTiO}_3$  substrate in the spectrum at  $V_g = -250$  V. Here we introduced in addition a polar  $\text{SrTiO}_3$  layer of thickness  $d_{\text{polar}}$  at the LAO/STO interface in which the *R*-mode is softened and split into two peaks. For this additional layer we used the same parameters for the soft mode and the stretching mode, whereas the layer thickness, the eigenfrequencies, width and the spectral weight of the *R*-modes were fitted. The optical response due to the additional LAO layer on top of STO was found to be vanishingly small in the relevant spectral range between  $410$  and  $460\text{ cm}^{-1}$  and therefore was neglected.

## Electric-field-induced anisotropy of the LO edge in LAO/STO heterostructures

The LO edge of the STO substrate in LS-5.5-1 at 10 K exhibits an electric-field-dependent unipolar change of the LO edge. As the polarity of the gate voltage is swept from  $V_g = +250$  V toward  $V_g = -250$  V, the LO edge of the STO substrate starts to shift toward higher energies and develops a feature which indicates an anisotropy of the LO edge. In Figure S4(a), the field-induced hardening of the LO edge is shown in terms of the ellipsometric angle,  $\Psi$ , for  $V_g \leq \pm 250$  V. It turns out that the properties of the LO

edge are closely related to the anomalous hardening of the soft-mode that is shown in Figures 1(h) and 1(i) in the manuscript.

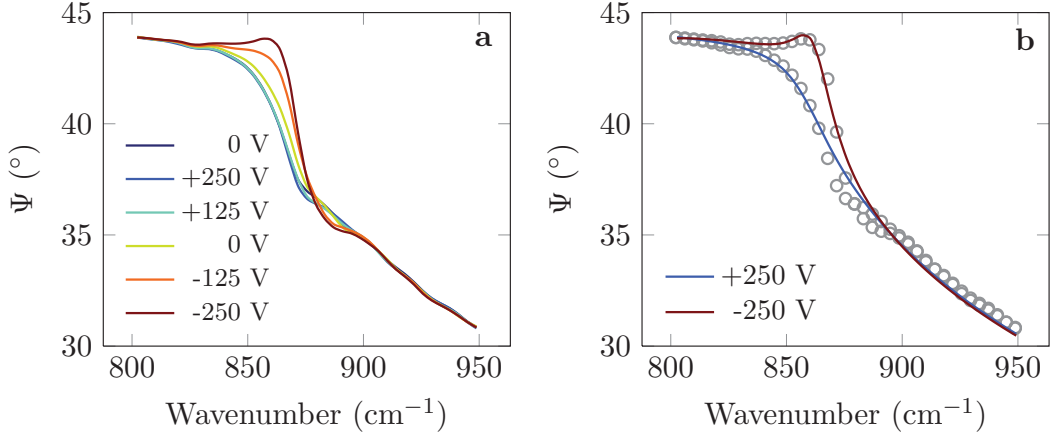


Figure S4: **a** Field-induced shift of the LO edge of the STO substrate in LS-5.5.1 at 10 K, shown in terms of the ellipsometric angle  $\Psi$ . **b** Comparison of the voltage-dependent experimental data (open symbols) and the model fit (solid lines) for  $V_g = +250$  V and  $V_g = -250$  V, respectively.

We have modeled the MIR spectra using a similar procedure as for the fitting of the FIR response in the vicinity of the  $R$ -mode. We assumed that the STO substrate of the heterostructure remains in the paraelectric phase at the positive gate voltage of  $V_g = +250$  V. This spectrum has been fitted first using a model dielectric function that consists of three Lorentz oscillators which account for the soft mode, the external mode, and the bending phonon mode of STO, respectively. The phonon modes are parametrised using values that have been obtained from the analysis of FIR ellipsometry spectra of another bulk  $\text{SrTiO}_3$  sample. At the negative gate voltage of  $V_g = -250$  V, a layer has been introduced on the STO side of the interface which accounts for the field-induced hardening of the soft mode eigenfrequency parallel to the field direction which is defined as the  $c$ -axis. The thickness of the interfacial layer has been fixed to the value of  $d_{\text{polar}} = 1 \mu\text{m}$  as obtained from the fitting of the FIR spectra. For the modelling of the MIR spectrum at  $V_g = -250$  V, the in-plane dielectric function of the polarized interfacial layer is assumed to be identical to the response of the paraelectric substrate at  $V_g = +250$  V. For the out-of-plane component of the dielectric function, the value of  $\varepsilon_{\infty,c}$ , the position  $\omega_c$ , and the spectral weight of the soft mode are fitted. This fit yields an anisotropy of the soft mode eigenfrequencies in the near interface region of the STO substrate corresponding to  $\omega_{a,b} = 18 \text{ cm}^{-1}$  and  $\omega_c = 19.8 \text{ cm}^{-1}$  which is consistent with the results from the analysis of the THz response shown in the manuscript in Figures 1(h) and (i). In Figure S4(b), the solid lines show the result of the model fit for  $V_g = \pm 250$  V,

respectively, which is compared to the measured data.

### Soft mode hardening in ferroelectric $\text{SrTi}^{18}\text{O}_3$

In the paraelectric state the peak position of the soft mode decreases from  $\sim 95 \text{ cm}^{-1}$  at 300 K to  $\sim 15 \text{ cm}^{-1}$  at low temperature [2, 3, 4]. In the pyroelectric state, the soft mode is expected to harden and to become anisotropic [5]. In the following we show that such a behaviour is observed in the ferroelectric phase of the  $\text{SrTi}^{18}\text{O}_3$  crystal with  $T^{\text{Curie}} = 23 \text{ K}$ . Figure S5 shows the conductivity spectra derived from a Kramers-Kronig transformation of reflectivity data. These confirm that the soft mode hardens by  $\sim 5 \text{ cm}^{-1}$  between 30 and 5 K. Similar values have been previously obtained from Raman measurements on  $\text{SrTi}^{18}\text{O}_3$  crystals [6].

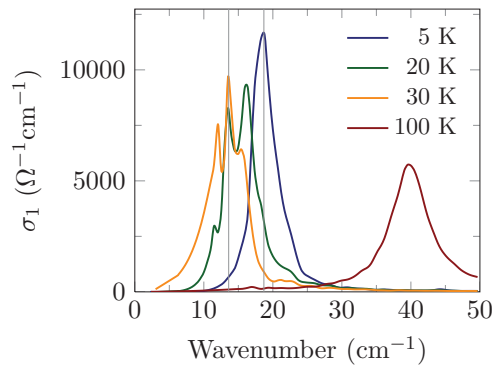


Figure S5: Optical conductivity spectra of the  $\text{SrTi}^{18}\text{O}_3$  crystal showing the soft mode softening in the paraelectric phase down to 30 K and the subsequent hardening at temperatures below  $T^{\text{Curie}} = 23 \text{ K}$ .

## References

- [1] Shigenari, T., Nakano, T. & Abe, K. Direction of polarization  $\vec{P}$  and the dipole interaction in the ferroelectric phase of SrTi<sup>18</sup>O<sub>3</sub>. *Europhys. Lett.* **94**, 57001 (2011).
- [2] Cochran, W. Crystal stability and the theory of ferroelectricity. *Adv. Phys.* **36**, 387–423 (1960).
- [3] Barker, A. S. & Tinkham, M. Far-Infrared Ferroelectric Vibration Mode in SrTiO<sub>3</sub>. *Phys. Rev.* **125**, 1527–1530 (1962).
- [4] Vogt, H. Refined treatment of the model of linearly coupled anharmonic oscillators and its application to the temperature dependence of the zone-center soft-mode frequencies of KTaO<sub>3</sub> and SrTiO<sub>3</sub>. *Phys. Rev. B* **51**, 8046–8059 (1995).
- [5] Yamanaka, A. *et al.* Evidence for competing orderings in strontium titanate from hyper-Raman scattering spectroscopy. *Europhys. Lett.* **50**, 688–694 (2000).
- [6] Takesada, M., Itoh, M. & Yagi, T. Perfect Softening of the Ferroelectric Mode in the Isotope-Exchanged Strontium Titanate of SrTi<sup>18</sup>O<sub>3</sub> Studied by Light Scattering. *Phys. Rev. Lett.* **96**, 227602 (2006).